Reactions of photogenerated fluorine atoms with dopant molecules in solid argon
1. Photolysis of solid Ar—$CH_4(CD_4)$—F_2 mixtures at 13—16 K

E. Ya. Misochko,[a] V. A. Benderskii,[a] A. U. Goldshleger,[a] A. V. Akimov,[a] A. V. Benderskii,[b] and C. A. Wight[b]*

[a]*Institute of Chemical Physics in Chernogolovka, Russian Academy of Sciences, 142432 Chernogolovka, Moscow Region, Russian Federation. Fax: 007 (095) 515 3588. E-mail: misochko@icp.ac.ru*

[b]*Department of Chemistry, University of Utah, Salt Lake City, Utah 84112, USA. Fax: +1 (801) 585 3207*

The products of UV photolysis of ternary Ar—$CH_4(CD_4)$—F_2 mixtures ($1 : c : c_0$, c, c_0 = 0.001—0.01) at 13—16 K were identified by ESR and FTIR spectroscopy. These products are $^{\cdot}CH_3$ ($^{\cdot}CD_3$) radicals of types I and II and molecular CH_3F—HF complexes. The latter were characterized by the IR bands of the stretching C—F (1003 cm^{-1}) and H—F (3774 cm^{-1}) vibrations. The ESR spectra of radicals I are asymmetric. The anisotropy of the g-factor ($\Delta g \approx 10^{-3}$) of radical I indicates that the structure of the radicals is nonplanar. The ESR spectrum of the type II radical is identical to that of matrix-isolated $^{\cdot}CH_3$ ($^{\cdot}CD_3$) radicals with the planar structure ($\Delta g < 5 \cdot 10^{-5}$). Under the experimental conditions, the amount of complexes formed in the photolysis is equal to $0.022 \cdot c$. When the photolysis is ceased, radical I disappears after ~10^3 s and radical II is stabilized. The limiting concentrations of the stabilized $^{\cdot}CH_3$ and $^{\cdot}CD_3$ radicals are equal to $2 \cdot 10^{-2} \cdot c$ and $2 \cdot 10^{-3} \cdot c$, respectively. A mechanism of the formation of the products is suggested. It is based on the assumption that both matrix-isolated CH_4 and F_2 and their heterodimers CH_4—F_2 are present in the samples and it takes into account the long-range migration of translationally excited flourine atoms. The CH_3F—HF complexes and radicals I are generated by the photolysis of the CH_4—F_2 heterodimers. The decay of radicals I is caused by geminate recombination of proximate F...CH_3 pairs. Radicals II are formed in the reaction of translationally excited fluorine atoms with isolated CH_4 (CD_4) molecules.

Key words: cryochemistry, photochemical reactions, methane, fluorine.

Crystals of inert gases have been previously used widely for spectroscopic studies of intermediate species and molecular complexes. In recent years, the dynamics of the elementary chemical reactions in these matrices has been studied, predominantly, by photodissociation of small molecules. Conventional experimental approaches combine time-resolved optical and IR spectroscopy with molecular dynamic (MD) simulation.[1—6] Among the results obtained in this field, the following data are noteworthy: the discovery of the high (close to unity) quantum yield of the photodissociation of F_2 molecules isolated in crystals of inert gases and the great thermalization length of translationally excited photogenerated fluorine atoms (up to 30 Å!) with initial excess energy $\Delta E_0 \geq 1$ eV.[3,4] This behavior of F atoms differs from that of atoms of other halogens formed in the photodissociation of Cl_2, Br_2, and I_2 in solid matrices. For these atoms, reverse cage recombination predominates, and the quantum yield of photodissociation of the molecules is not greater than 10^{-3}.[1,5] Another specific feature of the behavior of F atoms in crystal is that their diffusion thaws at temperatures above 20 K, which results in their recombination after 10^2—10^3 s.[3] Two temperature regions can be distinctly seen. Below 20 K only translationally excited ("hot") F atoms can move in space, while at 20—28 K thermal atoms recombine in the diffusion regime. In the Kr crystal, this transition occurs at 13—16 K.[3]

The long-range migration of translationally excited and thermal F atoms creates conditions in which they can interact with various doped molecules trapped in the inert matrix. Although the energetics of such reactions differs slightly from that for the gas phase, the crystalline environment prevents separation of the products and allows fast relaxation of the released energy. These specific features make it possible to stabilize intermediate species and their complexes with other products that cannot be detected in the gas phase. Ternary Ar—F_2—

Translated from *Izvestiya Akademii Nauk. Seriya Khimicheskaya*, No. 4, pp. 709—717, April, 1997.

1066-5285/97/4604-0678 $18.00

C_2H_4 mixtures have been studied as a model for the investigation of solid-phase reactions involving F atoms.[7,8] It has been established by ESR and FTIR spectroscopy that at $T < 20$ K the UV photolysis of F_2 molecules results in (a) the reaction of the two atoms in the complexes formed with the reagents (F_2—C_2H_4) to form molecular products:

$$[F_2 + C_2H_4] \xrightarrow{h\nu} [C_2H_3F + HF] + [C_2H_4F_2], \quad (1)$$

and (b) the reaction of one "hot" atom with an isolated C_2H_4 molecule to generate a stabilized radical

$$F + C_2H_4 \longrightarrow {}^{\cdot}C_2H_4F. \quad (2)$$

The ratio of the concentrations of the products of reactions (1) and (2) is equal to ~10 : 1, *i.e.*, the molecular products of cage reaction (1) predominate. At $T > 20$ K, by contrast, the reaction involving diffusing atoms (2) predominates, which results in the transformation of ~20% of the C_2H_4 molecules to stabilized ${}^{\cdot}C_2H_4F$ radicals. The absolute intensities of 8 vibrational bands of the radical were identified and measured for the first time by comparison of the kinetic data obtained by ESR and IR spectroscopy.

The preliminary ESR studies of the Ar—F_2—CH_4 and Ar—F_2—CD_4 mixtures testify that the ${}^{\cdot}CH_3$ and ${}^{\cdot}CD_3$ radicals are generated in the reactions of both "hot" (at $T < 20$ K) and thermal (at $T > 20$ K) atoms.[9,10] At the same time, the earlier IR spectroscopic studies showed[11] that the main products of the low-temperature photolysis of these mixtures are molecular CH_3F—HF complexes. These data allow one to conclude that the two channels of transformations (1) and (2) described above take place in the reactions of "hot" F atoms with CH_4 as well. The formation of ${}^{\cdot}CH_3$...${}^{\cdot}CH_3$ radical pairs and CH_3F—HF complexes that have been established previously for the photolysis of fluorine in methane crystals confirms these conclusion.[12—14]

In this series of works, we intend to measure the ratios between the main channels of transformations in the reactions of "hot" and thermal F atoms with various doped molecules in solid ternary Ar—F_2—X mixtures, as well as to elucidate the differences between the interactions of "hot" and thermal atoms. In this work, the photolysis of fluorine in Ar—$CH_4(CD_4)$—F_2 mixtures was studied by ESR and IR spectroscopy at temperatures of 13—16 K, *i.e.*, under the conditions in which the diffusion of thermal atoms is frozen. The approaches to studying the dynamics of solid-phase atomic-molecular reactions were based on the analysis of the data obtained and the results of the previous studies.[7—10]

Experimental

Samples were prepared by the combined condensation *in vacuo* of two gaseous Ar—$CH_4(CD_4)$ and Ar—F_2 mixtures onto a substrate cooled to 13—16 K. The rate of condensation of gases was equal to 15 μm min^{-1}. Ar—CH_4—F_2 samples of compositions 1 : c : c_0 (c, c_0 = 0.001—0.01) were studied. The samples with $c = c_0 = 0.001$ were studied in most detail. The samples were ~100 μm thick.

IR spectra were recorded on a Mattson Model RS/1000 FT-spectrometer with a resolution of 0.5 cm^{-1}. In these experiments, an APD Cryogenic Model helium refrigerator with a closed cycle was used, and the minimum working temperature on the CsI optical substrate was 16 K.

ESR measurements were carried out using a flow-type cryostat with a moving helium channel (Fig. 1). Gases were condensed on the lower end of a planar sapphire rod from two separate jets. To retard the reaction in the gas phase, gas flows were crossed directly near the substrate surface. After spraying, the rod with the sample was placed in the cavity of an ESR spectrometer. The temperature was measured with a thermocouple fixed at the upper end of the rod. In the preliminary calibration, the temperature of the lower end of the rod (at the site of condensation of the gases) was measured by a second thermocouple. For this purpose, an internal ESR standard (diphenylpicrylhydrazyl (DPPH) crystal) with a known number of spins (10^{12}) glued on the rod surface was used. These experiments showed that the difference in the temperatures monitored by the two thermocouples did not exceed 0.3 K in the interval of 10—30 K, and the intensity of the ESR line of the DPPH crystal I_s (the linewidth was <0.5 G) varied with the temperature measured by the upper thermocouple in accordance with the Curie law ($I_s \propto 1/T$). The thermoregulating system made the working temperature in the 13—30 K range stable with an accuracy of 0.1 K. The concentrations of the radicals were determined by comparing the integral intensities of the ESR spectra with that of the internal standard. The sensitivity of the measurements was not worse than ~10^{10} ${}^{\cdot}CH_3$ radicals per sample.

Fluorine atoms were generated by photolysis of F_2 using UV lasers with wavelengths of 335 nm (radiation of the third harmonic of a Nd : YAG laser with a frequency of 10 Hz in IR measurements) and 337 nm (radiation of an N_2 laser with a frequency of 1000 Hz in ESR measurements). The average power of the radiation was not greater than 10 mW cm^{-2}. Photodissociation of F_2 by light with these wavelengths gave

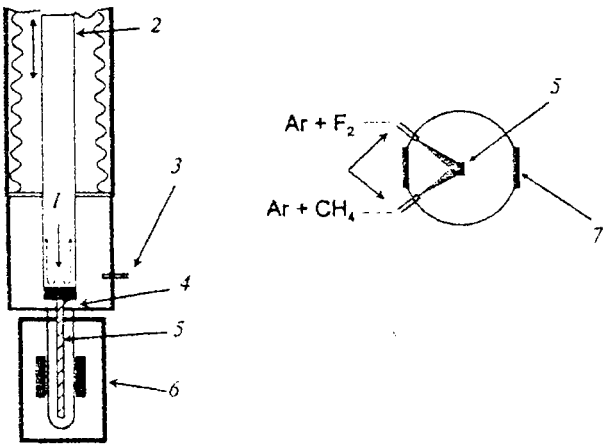

Fig. 1. Scheme of the ESR cryostat and preparation of samples: *1*, flow of gaseous helium, *2*, mobile helium blend, *3*, nozzles for spraying, *4*, thermocouple, *5*, sapphire rods, *6*, ESR cavity, and *7*, window.

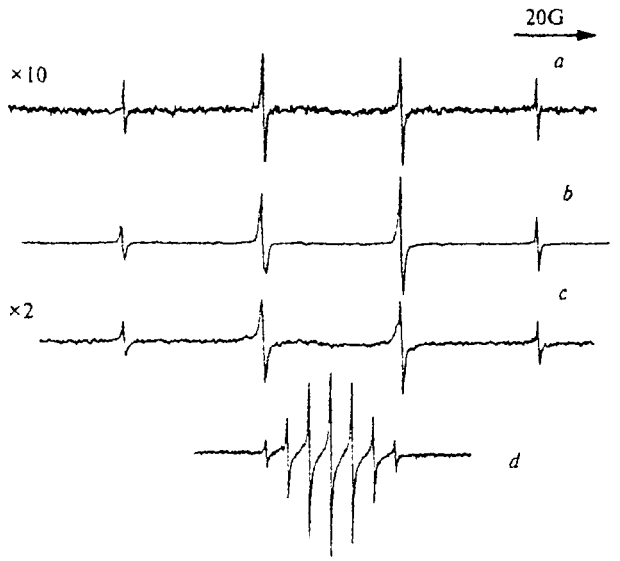

Fig. 2. ESR spectra of the $^{\cdot}CH_3$ radical at 13 K after preparation of the 1000 : 1 : 1 Ar—CH_4—F_2 sample (*a*); after photolysis (*b*); after completion of the dark reaction (*c*); spectrum of $^{\cdot}CD_3$ after completion of the dark reaction in the 1000 : 1 : 1 Ar—CD_4—F_2 sample at 13 K (*d*).

two "hot" F atoms with an additional translational energy $\Delta E_0 = (h\nu - D)/2 \approx 1$ eV per atom. The quantum yield of photodissociation of F_2 molecules isolated in solid argon was taken as $\Phi_0 = 0.35$ according to the published data.[3]

Results and Discussion

The characteristic bands of the molecular reaction products (see below) are almost absent in the IR spectra of the samples before photolysis. However, the ESR spectra indicate a small number of $^{\cdot}CH_3$ radicals ($\sim 10^{13}$ cm^{-3}), whose concentration 2—3 times changes depending on the conditions in which the samples were prepared and the amount of reagents in the gas flows.

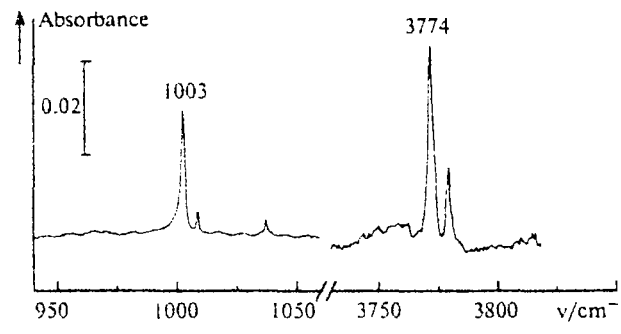

Fig. 3. IR absorption spectra of Ar—CH_4—F_2 samples (1000 : 1 : 1) in the range of vibrations of C—F and H—F after photolysis at 16 K.

The ESR spectrum of the $^{\cdot}CH_3$ radicals, which contains four symmetric lines of hyperfine structure with splitting of 23 G on three equivalent protons, is presented in Fig. 2, *a*. The linewidth is equal to 0.3—0.6 G, and the ratio of the integral intensities of the lines is equal to 1 : 3 : 3 : 1. No $^{\cdot}CD_3$ radicals were detected in the ESR spectra of the Ar—CD_3—F_2 mixtures.

At 16 K, photolysis of the samples containing F_2 and CH_4 molecules results in the appearance of an intense line at 1003 cm^{-1} in the the C—F vibration range and lines at 3774 and 3779 cm^{-1} in the region of HF vibration. The IR spectra of the products shown in Fig. 3 agree well with those presented previously.[11] The lines at 1003 and 3779 (3774) cm^{-1} were assigned[11] to C—F (ν_3) and HF vibrations in two configurations of the CH_3F—HF complexes. The formation of these complexes with these characteristic IR bands has been established[15] for the low-temperature condensation of the products of the gas-phase reaction of F atoms with CH_4 in excess argon.

Consumption of the methane molecules was monitored by the change in the intensity of the ν_3 band (1307 cm^{-1}). In the Ar—F_2—CH_4 (1000 : 1 : 1) samples, the maximum decrease in the intensity of this band after prolonged photolysis is equal to ~2.2%. It has been determined from the measured absolute intensity of the ν_3 band of the CH_3F molecule ($12 \cdot 10^6$ cm mol^{-1})[13] and the known initial number of molecules in the samples that the consumption of CH_4 molecules corresponds to the number of CH_3F molecules formed with an accuracy of 20%. This result confirms quantitatively the previous conclusion[11] that CH_3F—HF complexes are the main product of the photolysis. Their quantum yield is equal to 0.3—1.0 based on the number of photons absorbed by the CH_4—F_2 dimers, whose amount was taken as 2.2%.

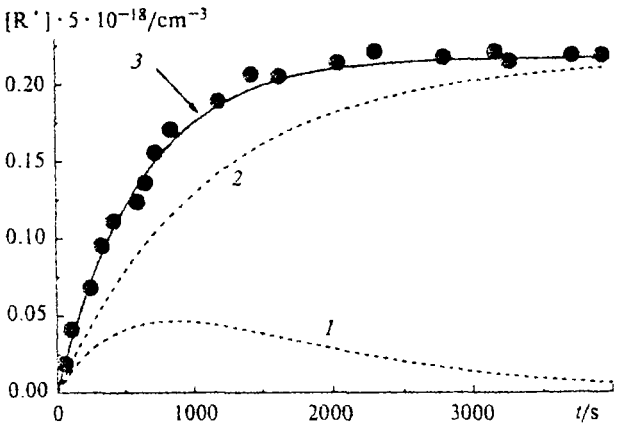

Fig. 4. Kinetics of the increase in the concentration of radicals during photolysis of the Ar—CH_4—F_2 sample (1000 : 1 : 1) at 13 K. Experiment is shown by points. Solutions of the system of equations (19) at $I = 3 \cdot 10^{17}$ cm^{-2}s^{-1} are shown by solid and dotted lines: *1*, $[R_I]$; *2*, $[R_{II}]$; and *3*, $[R_I + R_{II}]$.

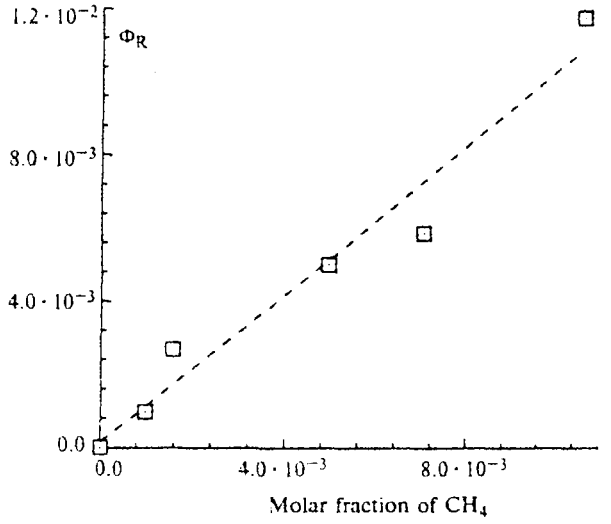

Fig. 5. Dependence of the quantum yield of radicals at 13 K on the concentration of CH_4 molecules (Ar—F_2, 1000 : 1).

Photolysis also results in fast accumulation of $^{\cdot}CH_3$ radicals. The ESR spectrum after a short period of (~300 s) photolysis is shown in Fig. 2, *b*. Unlike the ESR spectrum of the radicals formed during the preparation of the sample, the spectrum of the radicals generated during photolysis is characterized by pronounced asymmetry of the individual components of the hyperfine structure and by greater linewidths (up to 0.9 G). The number of radicals is proportional to the radiation dose $D_t = I \cdot t$ (where t is the time of photolysis) at the initial stages of the photolysis and reaches a maximum value after prolonged irradiation (Fig. 4). In the Ar—CH_4—F_2 (1000 : 1 : 1) samples, the limiting concentration of radicals relative to the initial number of CH_4 molecules is equal to $\sim 2 \cdot 10^{-3}$. No radicals are formed in samples containing no F_2 molecules. The concentration of radicals increases proportionally to the number of F_2 molecules when the amount of CH_4 in the samples is the same. This indicates that the radicals are generated due to absorption of light by the F_2 molecules. The quantum yield of the radicals is determined by the correlation

$$\Phi_R = (d[R]/dt)/\sigma I N_F, \quad (3)$$

where [R] is the concentration of the radicals, I is the intensity of the radiation, $\sigma = 1.05 \cdot 10^{-20}$ cm^2 and N_F are the absorption cross section and the initial concentration of F_2, respectively. The Φ_R value in the temperature range from 13 to 16 K is proportional to the mole fraction of CH_4 molecules (Fig. 5):

$$\Phi_R = (1.1 \pm 0.2) \cdot c. \quad (4a)$$

The change in the concentration of radicals [R](t) after photolysis is stopped is shown in Fig. 6. A portion of the radicals decay in the dark reaction at 13 K for $\sim 10^3$ s. The relative decrease in [R] reaches 30—50% in different experiments. Taking into account the radicals decaying in the dark reaction, the quantum yield of the radicals stabilized at the initial stage of the photolysis can be written as

$$\Phi_2 = (0.7 \pm 0.2) \cdot c. \quad (4b)$$

The ESR spectrum of the $^{\cdot}CH_3$ radicals remaining after the dark reaction is presented in Fig. 2, *c*. It follows from a comparison with the spectra presented in Figs. 2, *a* and 2, *b* that the stabilized radicals, like the radicals formed during the preparation of the sample, give narrower and more symmetric lines of the hyperfine structure than the radicals that disappear in the dark reaction.

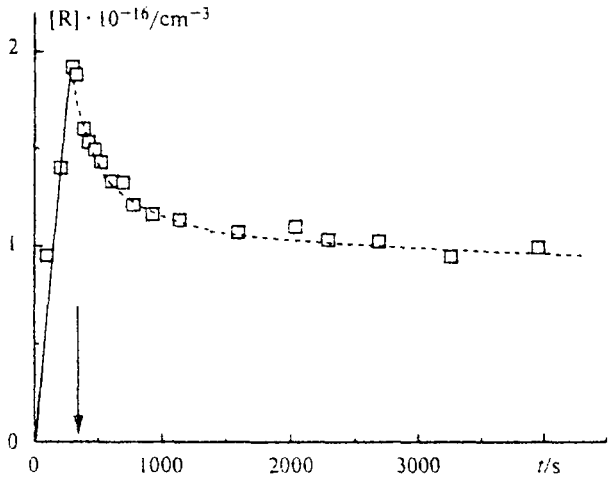

Fig. 6. Changes in the concentration of radicals during photolysis and dark reaction at 13 K. The moment of cessation of photolysis is shown by the arrow.

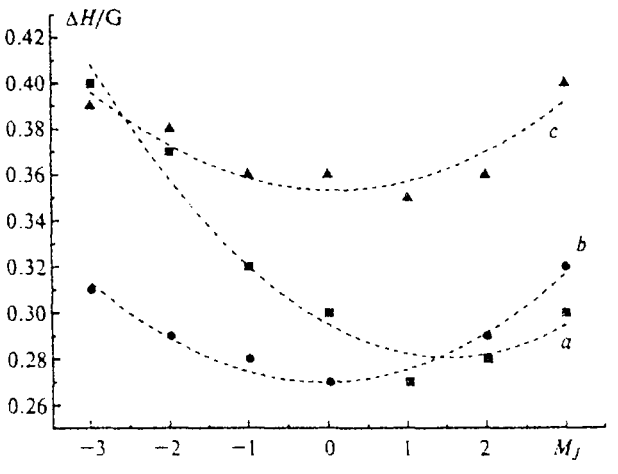

Fig. 7. Linewidths (ΔH) of the ESR spectrum of the $^{\cdot}CD_3$ radical corresponding to different projections of the total nuclear spin (M_J): after photolysis at 13 K (*a*); after heating to 20 K (*b*); after reverse cooling to 13 K (*c*).

The ESR spectrum of the stabilized $^{\cdot}CD_3$ radicals obtained after the photolysis of the $Ar-CD_3-F_2$ mixtures is shown in Fig. 2, *d*. The spectrum consists of seven lines of the hyperfine structure with splitting of 3.5 G; the ratio of the integral intensities of the lines is 1 : 3 : 6 : 7 : 6 : 3 : 1. The quantum yield of $^{\cdot}CD_3$ radicals is ~2.5 times lower than that of $^{\cdot}CH_3$ radicals in mixtures of similar compositions:

$$\Phi_R = (0.43 \pm 0.15) \cdot c. \qquad (5)$$

As in the mixtures with CH_4, ~30—40% $^{\cdot}CD_3$ radicals decay after ~10^3 s in the dark reaction. The ESR spectrum of the stabilized radicals has a different ratio of the intensities of the lines than the spectrum of the radicals formed in the photolysis, which is caused by changes in the linewidths. The linewidths of the spectrum of the $^{\cdot}CD_3$ radicals formed after a short period of photolysis and after the dark reaction can be seen in Fig. 7. The half-width of the lines changes as the total nuclear spin M_J increases from 0.28 to 0.4 G. These changes are more noticeable for the radicals generated after the short photolysis period.

Experiments on continuous saturation of the ESR lines of the $^{\cdot}CH_3$ and $^{\cdot}CD_3$ radicals were performed in order to determine the magnetic relaxation times t_1 and t_2. The measurements were carried out at 13 K after the dark reaction was completed and all F atoms had decayed at 24 K (the short time of the dark reaction at 13 K does not allow the exact values of t_1 and t_2 to be determined for decaying radicals). The curves of saturation of the $^{\cdot}CH_3$ and $^{\cdot}CD_3$ lines corresponding to different values of the projection of the total nuclear spin on the magnetic field direction M_J are presented in Fig. 8. The measured and theoretically predictable dependences of the intensity of the uniformly broadened differential lines I on the microwave field strength H_1 are presented in Fig. 8 as well:[16]

$$I \approx \frac{H_1}{\left(1 + \gamma_e^2 t_1 t_2 H_1^2\right)^{3/2}}. \qquad (6)$$

At 13 K, all lines of the $^{\cdot}CD_3$ radical and the lines of $^{\cdot}CH_3$ with $M_J = \pm 3/2$ are uniformly broadened. The lines of $^{\cdot}CH_3$ with $M_J = \pm 1/2$ are broader than those with $M_J = \pm 3/2$. At high UHF powers, their saturation curves decay more slowly than the saturated curves calculated from Eq. (6) (due to the contribution of the nonuniform broadening). These lines are the superposition of the components with $J = 1/2$ and $J = 3/2$ (J is the total spin of three protons, and the intensities of the components are equal to 2 and 1, respectively). The positions of the centers of these components differ due to the second-order correction (see, *e.g.*, Ref. 16):

$$H = H_0 \pm \frac{a}{2} - \frac{a^2}{2H}\left[J(J+1) - M_J^2\right], \qquad (7)$$

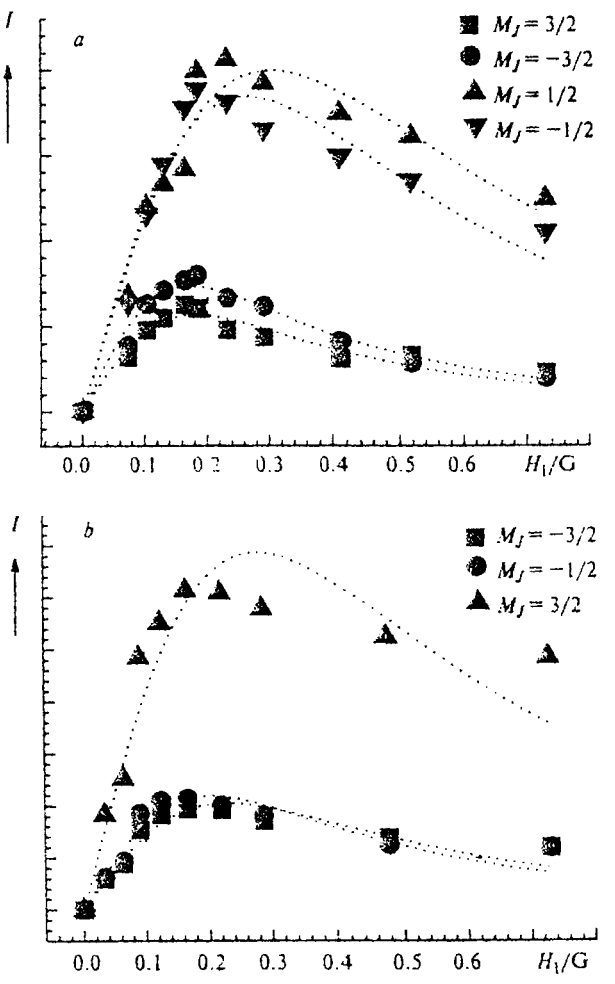

Fig. 8. Dependence of the intensity (I) of the lines of the ESR spectrum of the $^{\cdot}CH_3$ radical on the microwave field strength H_1 at $T = 13$ (*a*) and 24 K (*b*).

where H_0 is the position of the resonance line when the hyperfine coupling (HFC) is not taken into account and a is constant of HFC with protons. The distance between the centers of the $M_J = \pm 1/2$ components with $J = 1/2$ and $J = 3/2$ (~0.25 G) is on the order of their inherent width, which results in an additional nonuniform contribution to the linewidth. For $^{\cdot}CD_3$, the second-order correction (~10^{-2} G) is much less than the linewidths. Therefore, the saturation of all lines is close to uniform.

The width of the uniformly broadened lines increases as the microwave field strength increases (see Ref. 16):

$$\Delta H_{max}^2 = \frac{4}{3\gamma_e^2 t_2^2} + \frac{4t_1}{3t_2} H_1^2, \qquad (8)$$

where γ_e is the gyromagnetic ratio of an electron. Dependence (8) describes well the change in the widths of the edge components of $^{\cdot}CH_3$ and all the lines of

$^{\cdot}CD_3$. It follows from the slope of the curves in Fig. 9 that $t_1 \approx t_2$ for both $^{\cdot}CH_3$ and $^{\cdot}CD_3$. This ratio between the t_1 and t_2 times is characteristic of the fast rotation accelerating the HFC anisotropy.[17] These values can be estimated from the value of the microwave field strength at which the amplitude of the lines reaches a maximum, $H^2_{1m} = 1/(2\gamma_e^2 t_1 t_2)$: for $^{\cdot}CH_3$, $t_1 \approx t_2 = 2 \cdot 10^{-7}$ s was obtained; for $^{\cdot}CD_3$, $t_1 \approx t_2 = 2.7 \cdot 10^{-7}$ s.

The linewidth decreases somewhat as the temperature increases and is independent of H_1 when $H_1 \leq 0.5$ G. Both these facts can be explained by an increase in the contribution of the nonuniform mechanism of broadening. The saturation curves correspond to lines with an envelope width that is ~2 times greater than the width of the uniform line (spin-package). The increase in the contribution of the nonuniform broadening is evidence that the spin-packages narrow with the temperature.

Analysis of ESR spectra and the rotational mobility of radicals. The existence of two types of $^{\cdot}CH_3$ radicals follows from the shape of the ESR spectra. Type I radicals are formed in the photolysis and disappear due to subsequent recombination in the dark reaction. Their ESR spectrum is strongly asymmetric. Type II radicals are stabilized in the matrix. Their ESR spectrum is identical to that of the matrix-isolated radicals. The ratio of the t_1 and t_2 times determined in the previous section for type II radicals suggests that the anisotropy of the spin interactions is averaged by fast noncoherent rotation. Let us identify the radicals of both types by analysis of the shape of their ESR spectra. When the rotation is fast, the linewidth corresponding to the total spin J (and its projection M_J) of a radical in which all nuclei are equivalent is determined by the Fraenkel—Freed formula:[18]

$$t_2^{-1} = t_{2,0}^{-1} + \frac{\tau_c}{1 + \omega_a^2 \tau_c^2}\left[A + BM_J + C\left(J(J+1) + \frac{5}{3}M_J^2\right)\right], \qquad (9)$$

where $t_{2,0}^{-1}$ unites the contributions to the linewidth that are not associated with rotation; τ_c is the rotational correlation time; $\omega_a \sim \gamma_e(\Delta a + \Delta g H)$, ω_a is the scale of the anisotropy of the resonance frequencies. When the rotation is rather fast ($\tau_c\omega_a < 1$), $t_2^{-1} \sim \tau_c$. The temperature narrowing of the uniform lines caused by a decrease in τ_c as T increases and the fact that t_1 and t_2 are equal confirm the fast rotation of radical II. In this case, the HFC anisotropy is averaged, and the lines have the Lorentz shape.[18] Coefficients A, B, and C in Eq. (9) are determined by the anisotropy of the HFC- and g-tensors:

$$A = \frac{\gamma_e^2 H_0^2}{45\left(g_\perp - g_\parallel\right)^2}, \qquad (10)$$

$$B = \frac{4\gamma_e^2 H_0^2}{45\left(g_\parallel - g_\perp\right)\left(a_\parallel - a_\perp\right)}, \qquad (11)$$

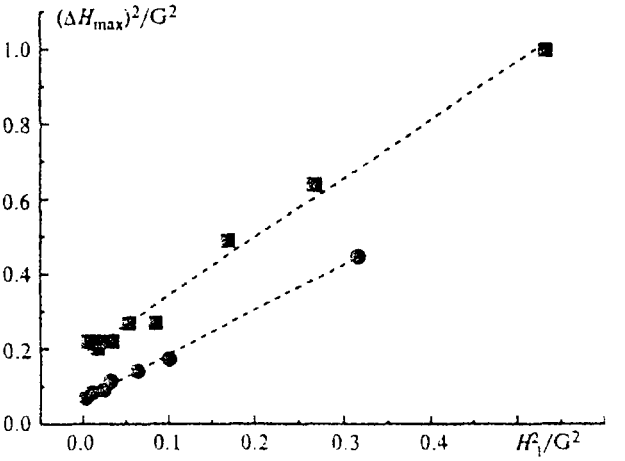

Fig. 9. Dependence of the linewidth $M_J = \pm 3/2$ of the $^{\cdot}CH_3$ radical on the microwave field strength H_1 at 13 K.

$$C = \frac{\gamma_e^2}{18\left(a_\parallel - a_\perp\right)}. \qquad (12)$$

Formula (9) predicts that the lines of the hyperfine structure of the radicals will have different widths. This can be seen in all ESR spectra observed (see Figs. 2 and 7). The dependences of the ESR linewidths of the $^{\cdot}CD_3$ radical on the projection of the total nuclear spin shown in Fig. 7 are well described by Eq. (9). The values of the $\tilde{B}$ and $\tilde{C}$ constants ($\tilde{B} = B\tau_c/\gamma_e$, $\tilde{C} = C\tau_c/\gamma_e$) determined by approximating the linewidths using a function in the form $\Delta H_{max} = \tilde{A} + \tilde{B}M_J + \tilde{C}M_J^2$ are the following: $\tilde{B} = 0.019$, $\tilde{C} = 0.0063$ G after photolysis at 13 K; $\tilde{B} = 0$, $\tilde{C} = 0.006$ G after decay of radicals I in the dark reaction; and $\tilde{B} = 0$, $\tilde{C} = 0.0045$ G at 20 K. The rotational relaxation time of $^{\cdot}CD_3$ is determined from the $\tilde{C}$ value by Eqs. (9) and (12). We did not find in the literature the value of the anisotropy HFC constant for $^{\cdot}CH_3$ or $^{\cdot}CD_3$, therefore, it was estimated from the McConnel formula:[19]

$$C = (1/5)\mu_D^2 \sum_{m=-2}^{2} D^{(m)} D^{(-m)} \approx 4\ \mathrm{G}^2, \qquad (13)$$

$$D^{(m)} = \sqrt{6\pi/5}\left\langle \psi \left| \frac{Y_{2,m}(\theta, \varphi')}{r^3} \right| \psi \right\rangle.$$

Here μ_D is the magnetic moment of a deutron; $D^{(m)}$ is the value of the constant of the dipole-dipole interaction between an electron and a proton averaged over the wave function of an electron; and Ψ is the normalized $2p_z$-wave function of an unpaired electron localized on the C atom. The rotational relaxation time (τ_c) was determined to be equal to $\sim 10^{-9}$ s.

The $^{\cdot}CH_3$ and $^{\cdot}CD_3$ radicals in the ground state are planar.[20—22] Due to the high symmetry, the anisotropy of the g-factor is very small and is not usually observed.

unlike that of the related $^{\cdot}SiH_3$ and $^{\cdot}GeH_3$ radicals.[23] The spectra of type II $^{\cdot}CH_3$ and $^{\cdot}CD_3$ radicals are perfectly symmetric, so the $\tau_c BM_J$ term is negligible, $\Delta g < 5 \cdot 10^{-5}$. Therefore, radicals II in the argon crystal remain planar. The HFC anisotropy and rotation cause the linewidths to be uniform. (Since the concentration of the radicals is low, the contribution of the electron dipole-dipole broadening can be neglected: $\Delta H_{d-d} = 2.5 \cdot 10^{-3}$ G.)

The spectra of type I $^{\cdot}CH_3$ and $^{\cdot}CD_3$ radicals are noticeably asymmetric, which, according to Eq. (9), is caused by the anisotropy of the g-tensor. Since the $\tilde{C}$ coefficients almost coincide for $^{\cdot}CD_3$ radicals of both types, the C values calculated from Eq. (12) are slightly sensitive to small distortions of the planar form of the radical, and the τ_c times are of the same order of magnitude for radicals I and II. The contribution of the anisotropy of the g-tensor ($\sim\Delta g M_J$) to the linewidths of the type I $^{\cdot}CD_3$ radical is greater than the effect of the anisotropy of the HFC-tensor. The $|\Delta g|$ value estimated from Eq. (11) is equal to $\sim 1-1.5 \cdot 10^{-3}$. The appearance of such substantial anisotropy of the g-tensor indicates that radical I in the Ar crystal becomes nonplanar. This value of Δg for radicals I coincides in order of magnitude with that of Δg for the $^{\cdot}SiH_3$ radical ($\Delta g \approx 3 \cdot 10^{-3}$)[23] in which the HSiH angle is ~113°.

The majority of small molecules (H_2, D_2, HX, CH_4), whose rotation constants are equal to ~5—10 cm^{-1}, rotate freely in matrices of inert gases.[24] Previously,[22] the IR bands observed in the region of the ν_2 vibration of the $^{\cdot}CH_3$-d_n radicals were assigned to different vibration-rotation transitions. The effect of coherent rotation on ESR spectra (magnetic-dipole transitions) should appear only as a correction to the g-factor, which depends on the rotation number N. The Hamiltonian that takes into account this correction to the electron Zeeman interaction has the form:[25]

$$\hat{H}_z = \mu_B \mathbf{H} \cdot (\hat{g}_s \hat{S} + \hat{g}_r \hat{N}), \qquad (14)$$

where $\hat{g}_r$ is the rotation g-factor, which is expressed through the spin-rotation and spin-orbital coupling constants:

$$g_r^{zz} = -\frac{|\varepsilon_{zz}|}{\xi}. \qquad (15)$$

The value of the spin-rotation constant for $^{\cdot}CH_3$ $\varepsilon_{zz} = -350$ MHz, $\varepsilon_{xx} = \varepsilon_{yy} = -3$ MHz, $\xi = 28$ cm^{-1},[26] which gives a correction to the g-factor $g_r^{zz} \approx 4 \cdot 10^{-4}$. This means that the population of the excited rotation levels should result in additional temperature broadening of the lines[27]

$$\Delta H_{max}^{(S,N)} \approx \left(g_r^{zz}\right)^2 \frac{\omega}{9\gamma_e} \langle N \rangle_T, \qquad (16)$$

where the $\langle N \rangle_T$ value is determined by the population of the rotation levels. At 13—20 K only the rotation levels with $N = 1$ and 2 are populated, so this effect is small for the $^{\cdot}CH_3$ and $^{\cdot}CD_3$ radicals and does not result in nonuniform broadening, which is caused rather by the nonequivalent positions of the radicals in the lattice. Thus, analysis of the ESR spectra of the radicals makes it possible to conclude that *photolysis of F_2 results in the formation of two types of radicals: nonplanar (type I), recombining after photolysis ceases and planar (type II), stabilized in the matrix.* Both types of radicals are characterized by fast rotation that averages the anisotropy of the HFC and the g-factor.

Reactions of "hot" atoms. The data presented show that there are two channels of the formation of products of the reactions of photogenerated atoms below 17 K. The main products are molecular CH_3F—HF complexes formed with the participation of two F atoms and one CH_4 molecule. At temperatures below 20 K, the diffusion of thermal atoms is frozen, so complexes of molecular products are formed with the participation of a pair of F atoms generated by photolysis of one molecule. The MD simulation showed[4] that when both "hot" atoms escape from the cage, they scatter in opposite directions. The probability that they would react with the same CH_4 molecule is close to zero. Therefore, CH_3F—HF complexes are formed only in the photolysis of heterodimers isolated in the matrix:

$$[F_2...CH_4] \xrightarrow{h\nu} [F^{\cdot} + F^{\cdot}...CH_4] \longrightarrow [CH_3F—HF]. \quad (17)$$

When the distribution of the reagents in the nodes of the argon fcc-lattice is random, the probability that CH_4 occupies one of the 12 nearest nodes that surround a node occupied by a F_2 molecule is equal to $12c$. However, the experimentally measured amount of molecular product is double this value. This means that a portion of the reagents form heterodimers upon condensation. This gives a number of matrix-isolated pairs of reagents ($CH_4...F_2$) that exceeds the statistical number. A similar effect has been observed previously[8] in ternary Ar—F_2—C_2H_4 mixtures. The intermolecular interaction in the C_2H_4—F_2 complex results in a considerable shift of the IR band of the ethylene molecules. Therefore, the complexes were distinguished from the isolated C_2H_4 molecules by spectral methods. In the photolysis of the samples, almost all complexes were transformed to the products of reaction (1) similar to process (17). Probably, the interaction in the CH_4—F_2 complexes is considerably weaker than in the previous case, and they cannot be distinguished spectrally from isolated CH_4 molecules. At the same time, the high yield of the products of reaction (17), which is close to the amount of CH_4 consumed, suggests that *as in the case of the (C_2H_4—F_2) complexes, photolysis of the F_2 molecules in the isolated pairs of reagents (CH_4—F_2) results in the predominant formation of molecular products.*

The radicals are formed in photolysis due to the reaction of one hot F* atom:

$$F^* + CH_4 \longrightarrow {}^{\cdot}CH_3 + HF. \qquad (18)$$

There are two possible routes of formation of radicals in low-temperature photolysis (*i.e.*, in the absence of diffusion of thermalized F atoms): (a) photolysis of the (CH_4—F_2) heterodimers in which one of the F atoms leaves the cage; (b) meeting of a "long-path" hot F atom with an isolated methane molecule. Channel (a) competes with reaction (17) and results in the formation of a radical, an HF molecule, and a hot F atom. When the latter is thermalized at the adjacent internode, its geminate recombination with the radical occurs to give molecular products (similar to reaction (17)). This route can be assigned to radicals **I**. Probably, the presence of a thermalized F atom in the vicinity of the radical is a reason for distortion of its planar structure, as has been concluded from the analysis of the ESR spectra. Radicals **II** can be formed *via* both channels when F atoms leaving the cage migrate further. Since the quantum yields of the photodissociation of isolated F_2 molecules (according to Ref. 3) and F_2 molecules in (F_2—CH_4) pairs are close ($\Phi_0 \approx 0.3$—0.5), the kinetic equations describing the changes in the concentrations of radicals **I** and **II** in the photolysis have the following form:

$$\left.\begin{aligned} d[F_2]/dt &= -\Phi_0 I \sigma [F_2], \\ d[R_{II}]/dt &= \Phi_2 I \sigma [F_2], \\ d[R_I]/dt &= \Phi_1 I \sigma [F_2] - k[R_I], \end{aligned}\right\} \qquad (19)$$

where k is the rate constant of geminate recombination ($k = 1.5 \cdot 10^{-3}$ s^{-1} at 13 K), $\Phi_1 = 4 \cdot 10^{-4}$ and $\Phi_2 = 7 \cdot 10^{-4}$ are the quantum yields at $c = 10^{-3}$ of radicals **I** and **II**, respectively.

It follows from Eqs. (19) that at $kt << 1$ radicals **I** and **II** are simultaneously accumulated, and at $kt >> 1$ only the concentration of radicals **II** increases and reaches a maximum $[R_{II}]_{max}$ when the F_2 molecules are completely consumed. There is a simple correlation between Φ_2 and $[R_{II}]_{max}$:

$$\Phi_2 = \Phi_0 \frac{[R_{II}]_{max}}{[F_2]_0}. \qquad (20)$$

The measured Φ_2 and $[R_{II}]_{max}$ values correspond to $\Phi_0 = 0.3$, which agrees with the published data.[3] The $[R_I](t)$ and $[R_{II}](t)$ dependences calculated from Eqs. (19) agree with the kinetics of radical accumulation (see Fig. 4). The relative probability of the channels of formation of radicals **I** (*i.e.*, CH_3(**I**)—F—HF) and molecular products CH_3F—HF in the photolysis of CH_4—F_2 heterodimers can be estimated as 0.02—0.06, comparing Φ_1 with the quantum yields of the molecular complexes.

The conditions of the reaction of "long-path" hot atoms with isolated CH_4 molecules (18) should depend on the character of migration of the atom through the crystal until it is thermalized. According to the MD simulation,[4] migration of the "hot" atom with $\Delta E_0 > 1$ eV is close to ballistic. The atom migrates to a great distance if it initially falls in the "escape cone" bounded by the "window" of D_3 symmetry of the first coordination sphere. In the opposite case, when the atom undergoes strong collisions with the nearest atoms of the lattice, it either remains at the initial node or is thermalized in the adjacent octahedral insertion sites. The Φ_2 value can be estimated using the effective cross section of the collision CH_4+F reaction in the gas phase $\sigma \approx 5 \cdot 10^{-16}$ cm^2 as the probability that at least one CH_4 molecule exists in the volume frequented by the migrating F atom. At $c << 1$

$$\Phi_2 \approx 2\Phi_0 \, c\sigma L_t N_0. \qquad (21)$$

When the mean length of thermalization of the hot atom $L_t \approx 20$ Å and $N_0 = 2.2 \cdot 10^{22}$ cm^{-3} (the number of Ar atoms in 1 cm^3), $\Phi_2 \approx 0.5 \cdot c$, which is close to the experimental value. This estimation indicates that stabilized radicals can be formed *via* channel (b) in reactions of "long-path" hot atoms. It is noteworthy that the ESR spectrum of the stabilized radicals contains no distortions caused by magnetic interactions with nuclei of the other product, HF molecules. If it stabilized near the radical (in the nearest octahedral or tetrahedral insertion sites at distances of 2.7—3.0 Å from the node occupied by the radical), its dipole-dipole interaction should result in splitting (or broadening) of the lines by 0.4—0.8 G. The fact that the ESR spectrum of stabilized radicals **II** is identical to the spectrum of matrix-isolated radicals indicates the spatial separation of the products of the reaction of the hot atom ($^{\cdot}CH_3$ and HF). The translationally excited HF molecules formed in the reaction leave the nearest neighborhood of the node, which was primarily occupied by the CH_4 molecule, and are stabilized beyond its first coordination sphere.

* * *

Combined application of IR spectroscopy and ESR demonstrates that it is possible to separate the cage reaction in heterodimers of reagents and the reactions involving "long-path" atoms. It is precisely the study of the latter which is of special interest because of the possibility of stabilizing the intermediate products of similar gas-phase reactions. Although the main photochemical reaction (17) results in the formation of molecular products, F atoms leave the cage with a probability of 0.02—0.06 and are thermalized at one of the nearest internodes. Decomposition of the cage also results in the formation of an HF molecule and radical **I** with a nonplanar structure. The geminate recombination of the F atom and radical **I** occurs in the time scale of 10^3 at considerably lower temperatures than thermoactivated diffusion of thermalized F atoms. This fact, as well as the differences in the ESR spectra of the radicals, made it possible to separate this radical channel from the formation of stabilized radicals **II**. The long-range migration of F atoms allows them to meet and react with isolated CH_4 molecules to form radicals **II**.

The ratio of the quantum yields of radicals I and II is independent of the concentrations of F_2 and CH_4 and can be estimated from the formula that follows from Eq. (21):

$$\frac{\Phi_2}{\Phi_1} \approx \frac{\sigma L_4 N_0}{K W_R}, \qquad (22)$$

where K is the fraction of the reagents bound in the heterodimers and W_R is the probability of cage breakage to form radical II. The experimental value $\Phi_2/\Phi_1 \sim 1$, in spite of the fact that $W_R << 1$. Correlation (22) shows that the reliable identification of radical reactions involving "long-path" atoms requires that the number of heterodimers of the reagents be decreased to the statistical limit, and the probability of cage breakage should be as small as possible.

The present work was financially supported by the Russian Foundation for Basic Research (Project No. 95-03-08509) and the National Science Foundation of the U.S. (NSF, Grant CHE-9300367).

References

1. V. E. Bondebey and L. E. Brus, *Adv. Chem. Phys.*, 1980, **41**, 269.
2. M. E. Fajardo and V. A. Apkarian, *J. Chem. Phys.*, 1986, **85**, 5660.
3. J. Feld, H. Kunti, and V. A. Apkarian, *J. Chem. Phys.*, 1990, **93**, 1009.
4. K. Alimi, R. B. Gerber, and V. A. Apkarian, *J. Chem. Phys.*, 1990, **92**, 3551.
5. J. G. McCaffrey, H. Kunz, and N. Schwentner, *J. Chem. Phys.*, 1992, **96**, 2825.
6. A. V. Danilychev and V. A. Apkarian, *J. Chem. Phys.*, 1994, **100**, 5556.
7. V. A. Benderskii, A. U. Goldschleger, A. V Akimov, E. Ya. Misochko, and C. A. Wight, *Mendeleev Commun.* 1995, **6**, 203.
8. E. Ya. Misochko, A. V. Benderskii, and C. A. Wight, *J. Phys. Chem.*, 1996, **100**, 4496.
9. E. Ya. Misochko, V. A. Benderskii, A. U. Goldschleger, and A. V. Akimov, *Mendeleev Commun.*, 1995, **5**, 198.
10. E. Ya. Misochko, V. A. Benderskii, A. U. Goldschleger, A. V. Akimov, and A. F. Shestakov, *J. Am. Chem. Soc.*, 1995, **117**, 11997.
11. G. L. Johnson and L. Andrews, *J. Am. Chem. Soc.*, 1980, **102**, 5736.
12. E. Ya. Misochko, V. A. Benderskii, A. U. Goldschleger, and A. V. Akimov, *Mendeleev Commun.*, 1994, **5**, 203.
13. E. Ya. Misochko and A. U. Goldschleger, *Dokl. Akad. Nauk*, 1994, **337**, 772 [*Dokl. Chem.*, 1994, **337** (Engl. Transl.)].
14. E. Ya. Misochko, V. A. Benderskii, and A. U. Goldschleger, *J. Phys. Chem.*, 1995, **99**, 13917.
15. M. E. Jacox, *Chem. Phys.*, 1979, **42**, 133.
16. J. Wertz and J. Bolton, *Electron Spin Resonance*, McCraw-Hill, New York, 1972.
17. A. Abragam, *The Principles of Nuclear Magnetism*, Clarendon Press, Oxford, 1961.
18. J. H. Freed and J. K. Fraenkel, *J. Chem. Phys.*, 1963, **39**, 326; J. K. Fraenkel, *J. Phys. Chem.*, 1967, **71**, 139.
19. H. McConnell and J. Strathdee, *Mol. Phys.*, 1959, **2**, 944.
20. M. J. Karplus, *Chem. Phys.*, 1959, **30**, 15.
21. R. W. Fessenden, *J. Phys. Chem.*, 1967, **71**, 74.
22. M. E. Jacox, *J. Mol. Spect.*, 1977, **66**, 272.
23. R. L. Morehouse, J. J. Christiansen, and W. Gordy, *J. Chem. Phys.*, 1966, **45**, 1751.
24. In *Inert Gases*, Ed. M. L. Klein, Springer, Berlin, 1984, 134.
25. C. E. Barnes, J. M. Brown, A. Carrington, J. Pinkstone, and T. J. Sears, *J. Mol. Spect.*, 1978, **72**, 86.
26. C. Yamada, E. Hirota, and K. Kawaguchi, *J. Chem. Phys.*, 1981, **75**, 5256; T. Amano, P. F. Bernath, C. Yamamada, Y. Endo, and C. Hirota, *J. Chem. Phys.*, 1982, **77**, 5284.
27. P. W. Atkins and D. Kivelson, *J. Chem. Phys.*, 1966, **44**, 169.

Received June 20, 1996;
in revised form October 25, 1996